

Refined Estimate of the Dominant T-Wave

Roberto Sassi¹, Luca T Mainardi²

¹Dipartimento di Tecnologie dell'Informazione, Università degli Studi di Milano, Crema, Italy

²Dipartimento di Bioingegneria, Politecnico di Milano, Milan, Italy

Abstract

The Dominant T-wave (DTW) offers an overall view of the ventricular repolarization as it reflects the first-order derivative of the transmembrane potential of the myocytes during repolarization (TMPR). DTW can be estimated from the analysis of surface T-waves, which are modeled as a linear combination of DTW and its derivatives. Usually, the contribute of the DTW dominates but, when dispersion of the repolarization times increases (as during pathological conditions) the effects of DTW derivatives can not be neglected. Unfortunately the estimators of DTW proposed so far, do not consider these terms.

In this work, an algorithm to estimate the DTW taking into account the second-order derivative of the TMPR curve is introduced. The algorithm was tested on synthetic ECG recordings. When the dispersion of the sources is varied from 10 to 50 ms, the new technique shows an average improvement in the precision of the estimate of the TMPR curve of about 18.9% over previous methods.

1. Introduction

The Dominant T-wave (DTW) was first introduced by van Oosterom [1] as a conceptual entity capable of explaining the empirical finding that T waves of all leads on the thorax seem, in a first approximation, a scaled version of a single waveform shape. Building on the work of Geselowitz [2] and assuming linearity of the conductive properties of the medium, van Oosterom showed that the potentials recorded at the skin during the repolarization phase of the ventricula can be approximated, using an equivalent surface source model (ESSM), by

$$\Psi = \mathbf{A} \begin{bmatrix} D(t - \rho_1) \\ \dots \\ D(t - \rho_M) \end{bmatrix}, \quad (1)$$

where Ψ is a $[L \times N]$ matrix containing the N ECG samples recorded from L leads while \mathbf{A} is a transfer $[L \times M]$ matrix which accounts for both the volume conductor (geometry and conductivity) and the solid angle under which the single source contributes to the potential Ψ . Matrix \mathbf{A}

is fixed for a given subject and a specific leads configuration. The function $D(t)$ is the repolarization phase of the transmembrane potential (TMPR) of the single myocyte which, for simplicity, is supposed to be identical across cells. The repolarization of each cell occurs with a time shift $\Delta\rho_m = \rho_m - \bar{\rho}$ where $\bar{\rho} = \sum_{m=1}^M \rho_m / M$ is the average repolarization time. From geometrical considerations, $\mathbf{A}e_1 = 0$ where e_1 is a $[M, 1]$ vector whose elements are all set to 1. Interestingly, the latter constrain on \mathbf{A} implies that there is a surface T-wave only if the repolarization times differ. To have a convenient model, groups of nearby myocytes are modeled as a single source. In here, M is the number of sources ("nodes") at the cellular level.

When $\Delta\rho_m \ll \bar{\rho}$, the function $D(t)$ can be expanded in series around $\bar{\rho}$ leading to

$$D(t - \rho_m) = D(t - \bar{\rho}) - \Delta\rho_m \left. \frac{dD(\tau)}{d\tau} \right|_{\tau=t-\bar{\rho}} + \frac{\Delta^2 \rho_m}{2!} \left. \frac{d^2 D(\tau)}{d\tau^2} \right|_{\tau=t-\bar{\rho}} + o(\Delta^3 \rho_m). \quad (2)$$

Given the fact that $\mathbf{A}e_1 D(t - \bar{\rho}) = 0$ and neglecting higher order terms, the model in equation (1) can be recast into

$$\Psi \approx -\mathbf{A} \begin{bmatrix} \Delta\rho_1 \\ \dots \\ \Delta\rho_M \end{bmatrix} \dot{D}(t - \bar{\rho}) + \frac{\mathbf{A}}{2} \begin{bmatrix} \Delta^2 \rho_1 \\ \dots \\ \Delta^2 \rho_M \end{bmatrix} \ddot{D}(t - \bar{\rho}). \quad (3)$$

A rank-1 approximation of Ψ is given by

$$\Psi \approx -\mathbf{A} \Delta \rho \dot{D}(t - \bar{\rho}) = w_1 T_d \quad (4)$$

where $w_1 = -\mathbf{A} \Delta \rho$ and the first derivative of the repolarization curve $\dot{D}(t - \bar{\rho})$ was termed by Van Oosterom dominant T-wave (T_d). In fact, when the approximation in equation (2) holds, the single T-waves measured on different leads are only a rescaled version of T_d . In the definition (4), the modules of both T_d and the lead factors w_1 are undetermined. Several routes might be followed; one is that of rescaling T_d such that its integral evaluates to the difference between the intracellular potential before (t_{de}) and after repolarization (t_{re}) which is typically 100 mV:

$$D(t_{de} - \bar{\rho}) - D(t_{re} - \bar{\rho}) = - \int_{t_{de}}^{t_{re}} T_d(\tau) d\tau = 100. \quad (5)$$

The apex of T_d as defined here might be negative.

Van Oosterom suggested to estimate T_d as the average of the potentials in Ψ weighted by their integrals $e_1^T \Psi^T$,

$$T_d^{VO} = c_1 e_1^T \Psi^T \Psi, \quad (6)$$

where the scalar c_1 is set using equation (5). He also noticed [3] that the series expansion in equation (3) is a composition of rank-1 matrixes, with some resemblances with the more classical rank-1 decomposition obtained through singular value decomposition (SVD),

$$\Psi = \mathbf{U} \mathbf{\Lambda} \mathbf{V}^T = \sum_{l=1}^L u_l \lambda_l v_l^T. \quad (7)$$

A check on 160 subjects [3] showed that a second estimate of the DTW obtained with $T_d^{R1} \propto v_1^T$ was highly correlated with T_d^{VO} . Also the singular vectors v_2^T and v_3^T were found correlated with higher (numerical) derivatives of T_d^{VO} .

When the dispersion of the repolarization times increases, as it is speculated in several pathological conditions like the long QT syndrome or when T wave alternance appears, the expansion in equation (3) breaks down and higher order contributions became relevant. Unfortunately so far no suggestions have been offered on how to take in account higher order derivatives in the estimate of the DTW.

In the following we suggest an algorithm to estimate the DTW taking into account the second-order derivative of the Tmpr curve as indicated in equation (12).

2. Methods

The correlation found by Van Oosterom between the two estimates T_d^{VO} and T_d^{R1} is not incidental and can be rationalized by observing that

$$\Psi^T \Psi = \mathbf{V} \mathbf{\Lambda}^2 \mathbf{V}^T = \sum_{l=1}^L \lambda_l^2 v_l v_l^T. \quad (8)$$

Then, if the singular values $\lambda_i \ll \lambda_1$ for $i \neq 1$,

$$e_1^T \Psi^T \Psi = \sum_{l=1}^L (\lambda_l^2 e_1^T v_l) v_l^T \approx (\lambda_1^2 e_1^T v_1) v_1^T. \quad (9)$$

When Ψ is actually a rank-1 matrix, the two estimates are identical, up to a scalar. Otherwise their similarity is constrained by how predominant is λ_1 over the other singular values. While we refer to the final discussion for a comparison of the two estimators, here we notice that T_d^{R1} is *optimal* in the sense that it minimizes the Frobenius norm of the error

$$\epsilon = \|\Psi - w_1 T_d\|_F, \quad (10)$$

thus offers (with w_1) the best rank-1 approximation to the matrix of the surface potentials. This claim follows directly from a classic result in linear algebra. By definition, the *best* rank-1 approximation to Ψ is the matrix Ψ_1 such that the Frobenius norm of the quadratic error

$$\epsilon = \|\Psi - \Psi_1\|_F \quad (11)$$

is minimum. But a classical theorem [4] states that $\Psi_1 = u_1 \lambda_1 v_1^T$. Then it must be $w_1 T_d = u_1 \lambda_1 v_1^T$. Multiplying both sides for u_1^T , we get $T_d \propto \lambda_1 / (u_1^T w_1) v_1^T$ where $\lambda_1 / (u_1^T w_1)$ is a constant factor.

A minimization of the Frobenius norm of the residual matrix, similar to equation (10), is commonly pursued in inverse electrocardiography. Coherently with this perspective, we suggest to find a DTW estimate which generalize this approach. Starting from equation (3), a rank-2 approximation Ψ_2 of Ψ is given by

$$\Psi \approx -\mathbf{A} \Delta \rho \dot{D}(t - \bar{\rho}) + 1/2 \mathbf{A} \Delta \rho^2 \ddot{D}(t - \bar{\rho}) \quad (12)$$

$$\Psi_2 = w_1 T_d + w_2 \dot{T}_d$$

where $w_2 = 1/2 \mathbf{A} \Delta \rho^2$. Then, we look for a vector T_d^{R2} which minimizes the Frobenius norm

$$\epsilon = \|\Psi - w_1 T_d - w_2 \dot{T}_d\|_F. \quad (13)$$

As before the optimal solution would be $\Psi_2 = w_1 T_d + w_2 \dot{T}_d = u_1 \lambda_1 v_1^T + u_2 \lambda_2 v_2^T$, but now this equation can not be solved directly as we can not force $T_d \propto v_1^T$ and $\dot{T}_d \propto v_2^T$ at the same time. Therefor the minimization of ϵ in the differential equation (13) must be enforced right away and several routes can be pursued. In here, we first exchange \dot{T}_d with a finite difference numerical approximation

$$\epsilon^2 = \sum_{i=1}^L \sum_{j=1}^N \{ \Psi_{i,j} - w_1(i) T_d(j) - w_2(i) [T_d(j+1) - T_d(j-1)] / (2\Delta t) \}^2 \quad (14)$$

and then take the partial derivatives of ϵ^2 with respect to $w_1(i)$, $w_2(i)$ and $T_d(j)$. The constant Δt is the inverse of the sampling rate as usual. The minimization results in solving a system of nonlinear equations in $2L + N$ unknowns but this difficulty can be overcome by iteratively solving two linear sub-parts of the system. In each iteration, an estimate for w_1 and w_2 is computed first by solving

$$\begin{cases} w_1 \|T_d\|^2 + w_2 \dot{T}_d T_d^T = \Psi T_d^T \\ w_1 \dot{T}_d T_d^T + w_2 \|\dot{T}_d\|^2 = \Psi \dot{T}_d^T. \end{cases} \quad (15)$$

Then a new value for T_d is obtained from

$$\begin{aligned} T_d(j) [\|w_1\|^2 + 2 \|w_2\|^2 / (2\Delta t)^2] & \quad (16) \\ + [T_d(j+2) - T_d(j-2)] \|w_2\|^2 / (2\Delta t)^2 = & \\ \sum_i \{ \Psi_{i,j} w_1(i) + [\Psi_{i,j-1} - \Psi_{i,j+1}] w_2(i) / (2\Delta t) \}. & \end{aligned}$$

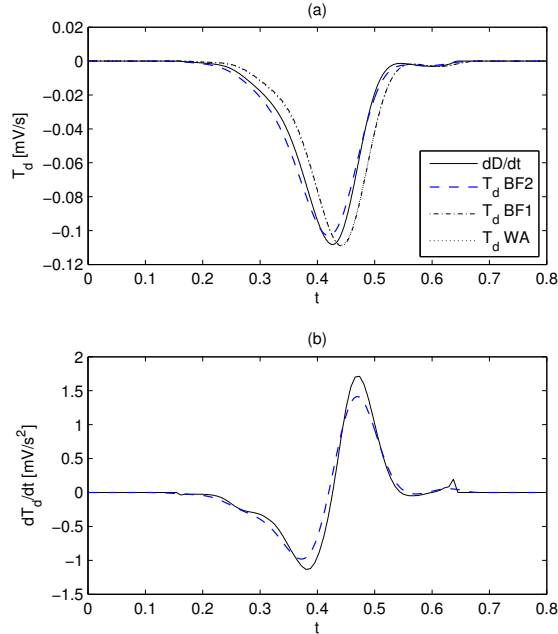


Figure 1. Panel (a). Three different estimates of the DTW T_d are compared with the first derivative of the TMPR $D(t)$ (continuous line). The simulation was performed with $\sigma_\rho = 20$ ms. Panel (b). Same as panel (a) but comparing the second derivative of the TMPR $D(t)$ with the first derivative of T_d , as estimated by method BF2.

Finally the two steps are iterated until the changes in the value of ϵ^2 between successive iterations is smaller than a predefined threshold (0.001 in the following). The two systems in equations (15) and (16) are banded diagonal and computationally efficient solvers do exist. We will term the value of T_d estimated with this method as T_d^{R2} .

The separate evaluation of w_1 and w_2 might seem questionable as they both depend on $\Delta\rho$. On the other hand, this appears reasonable if one considers that: (i) if the values $\Delta\rho_m$ are independent random variables, then it can be shown that the linear correlation of w_1 and w_2 is actually zero. (ii) in practical situations, where the changes in repolarization times of nearby cells are coupled, the large number of sources in $\Delta\rho$ makes w_1 and w_2 *practically* uncorrelated.

To test the new algorithm and to compare it with the other two DTW estimates we discussed in the introduction, synthetic surface ECG T-waves were generated. Equation (1) was used to generate the potentials Ψ . In this way a direct comparison could be established with the derivative of the TMPR $D(t)$. The scaling factors \mathbf{A} which accounts for the geometry of the sources were derived from ECGSIM [5], a freely available software implementing the ESSM of equation (1). We only considered 8 independent leads among the 12 standard ones. In this configuration,

the matrix \mathbf{A} linked the effect of 257 sources on 8 surface potentials. Also the shape of the repolarization curve was taken from ECGSIM and approximated with a spline model to make possible shifts below 1 ms.

The average repolarization delay $\bar{\rho}$ was kept fixed during the simulation, while the repolarization time of each node was set to be $\rho_m = \bar{\rho} + \varphi_m$, where φ_m are independent zero-mean normal random variables $\sim \mathcal{N}(0, \sigma_\varphi^2)$. The standard deviation σ_φ determines the dispersion of the repolarization times. When $\sigma_\varphi = 0$ no T wave is observable at the skin.

For each potential Ψ , the DTW was estimated with T_d^{VO} , T_d^{R1} and the newly introduced T_d^{R2} . The three estimates were compared with the effective value of $\dot{D}(t)$ derived from the function $D(t)$ used in the model (1). The goodness of the estimates was quantified by (i) the squared error ζ^2 , computed over the differences between $\dot{D}(j\Delta t)$ and any T_d ; and (ii) the correlation coefficient among $\dot{D}(j\Delta t)$ and any T_d . Each of the DTW estimates and $\dot{D}(j\Delta t)$ were rescaled to unit norm before the comparison. The dispersion of the repolarization times σ_φ was increased on a logarithmic scale from 0.1 ms to 1 second and, for each value of σ_φ , the procedure was repeated 40 times to ensure statistical convergence.

3. Results

In figure (1) the three estimates of the DTW are displayed along with the curve $\dot{D}(t)$ (panel a) for a case where $\sigma_\varphi = 20$ ms. While T_d^{VO} and T_d^{R1} are nearly indistinguishable, T_d^{R2} gets closer to the effective value of the derivative of the TMPR. Panel (b) shows the second derivatives; the large amplitudes reached by $\ddot{D}(t)$ hint significant effects on Ψ when w_2 is not negligible.

Figure (2) report the values of the squared error ζ^2 and the correlation coefficients varying with σ_φ . For values of $\sigma_\varphi < \approx 5$ ms the three estimates are mainly indistinguishable. On the contrary for $\sigma_\varphi > 5$ ms the estimated provided by T_d^{R2} are generally more precise than the others two. On average, when the dispersion of the sources is in the physiologically relevant range of 10 to 50 ms, the new technique T_d^{R2} shows an improvement of about 18.9% over previous methods. Finally, for $\sigma_\varphi > \approx 70$ ms, the contribution of the second order terms becomes comparable to first order ones and the expansion (3) breaks down. The estimates provided by T_d^{R2} are yet better than those obtained through the other two methods, but the shape of T_d starts departing from $\dot{D}(t)$ (the correlation coefficient lowers below 0.9 for all methods). In these last situations, the increased computational burden of T_d^{R2} over T_d^{VO} might be questionable for the little accuracy gained.

These results can be rationalized as follows. Under the hypothesis that the delays $\Delta\rho_m$ are independent normal random variables, it can be proven that $E[|w_2(i)|] =$

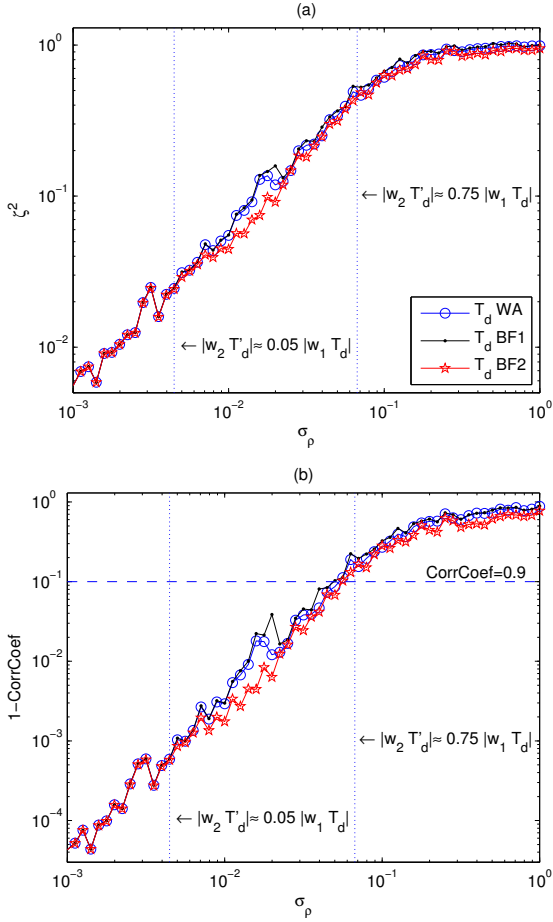


Figure 2. Panel (a): Average squared error ζ^2 estimating the DTW. Panel (b): Average correlation coefficients.

$\sigma_\varphi/\sqrt{2}E[|w_1(i)|]$ (see next section). We might expect the second order term in eq. (12) to start being not-negligible approximately when $|w_2(i)| \max_t |\dot{T}_d| > \gamma |w_1(i)| \max_t |T_d|$ (being γ a small number), that is when $\sigma_\varphi > \gamma \sqrt{2} \max_t |T_d| / \max_t |\dot{T}_d|$. In figure (2) we add a pair of vertical dotted lines corresponding to $\gamma = 5\%$ and $\gamma = 70\%$. The theoretical prediction matches the results of the simulations very well.

4. Discussion and conclusions

The values in **A** make the contribution of each node on Ψ different, therefore for a given σ_φ a large T wave variability is displayed. As a consequence the results discussed here are related to the average performances of the estimators. The work showed that DTW estimates which take into account only the first derivative of the TMPR are nearly equivalent with a slighter accuracy of T_d^{VO} over T_d^{R1} . This might be rationalized considering equation (9): T_d^{VO} is affected by every singular value and this turns rel-

evant when the first one is not predominant.

The three methods give estimates which are indistinguishable for small values of σ_φ . But when the dispersion of the sources is increased over 10 ms, T_d^{R2} offers, on average, better estimates. We think that it might permit to employ the DTW formalism in a larger set of applicative contexts.

As a final remark, we notice that the method we suggested in this work, a part from being a better alternative for the estimate of the DTW, permits an assessment of the dispersion of repolarization times σ_φ . We only sketch here the main idea, which is valid only under the assumption made in this paper, that the times $\Delta\rho_m$ are independent normal random variables $\sim \mathcal{N}(0, \sigma_\varphi^2)$. While this might be limited, it is still a starting point for future improvements. Under this hypothesis, it can be proven that $w_1(i)$ is a normal random variable $\sim \mathcal{N}(0, \sigma_\varphi^2 \sum_m A_{i,m}^2)$. On the other hand, $w_2(i)$ is a linear combination of chi-squared random variables (1 degree of freedom). But M is large and for the central limit theorem, $w_2(i)$ is also approximately normal with $\sim \mathcal{N}(0, \sigma_\varphi^4 \sum_m A_{i,m}^2/2)$. The standard deviation of $w_2(i)$ depends quadratically on σ_φ , while that of $w_1(i)$ only linearly. Therefore, one can assess $\sigma_\varphi = \sqrt{2} \text{std}[w_2(i)]/\text{std}[w_1(i)]$, where $\text{std}[\cdot]$ is the sample standard deviation.

Acknowledgements

RS is grateful to T.F. Oostendorp for clarifications on ECGSIM.

References

- [1] van Oosterom A. Genesis of the T wave as based on an equivalent surface source model. *J Electrocardiol* 2001;34 Suppl:217–227.
- [2] Geselowitz D, Miller W. A bidomain model for anisotropic cardiac muscle. *Annals of Biomedical Engineering* 1983; 11:191–206.
- [3] van Oosterom A. Singular value decomposition of the T wave: Its link with a biophysical model of repolarization. *Int J Bioelectromagnetism* 2002;4:59–60.
- [4] Leon SJ. *Linear Algebra with Applications*. 6^{ed} edition. Prentice Hall, 2006.
- [5] van Oosterom A, Oostendorp TF. ECGSIM: an interactive tool for studying the genesis of QRST waveforms. *Heart* 2004;90:165–168.

Address for correspondence:

Roberto Sassi
 Dipartimento di Tecnologie dell'Informazione
 Università degli Studi di Milano
 via Bramante 65, 26013 Crema (CR) Italy
 E-mail address: roberto.sassi@unimi.it